Egypt. J. Chem. **Vol. 63,** No.6, pp. 2331 - 2344 (2020)

Egyptian Journal of Chemistry
http://ejchem.journals.ekb.eg/

Enhancement of Photocatalytic Activity for Nanostructured ZnO Thin Film Prepared by Pulsed Spray Pyrolysis

M. Obaida[1], I. Moussa[1], S. A. Hassan[1], H. H. Afify[1] and A. Abouelsayed[2]*
[1]Solid State Physics Department, Physics Division, National Research Centre, 33 El Bohouthst. (former El Tahrirst.) - Dokki - Giza - P.O. 12622 -Egypt.
[2]Spectroscopy Department, Physics Division, National Research Centre, 33 El Bohouthst. (former El Tahrir St.) - Dokki - Giza - P.O. 12622 - Egypt.

SIMPLE pulsed spray pyrsolysis (PSP) technique is used to prepare pure nanostructured zinc oxide (ZnO) thin films at different deposition temperatures and spraying times on glass substrates. XRD measurements show polycrystalline ZnO hexagonal wurtzite phase preferably oriented perpendicular through c- axis along (002) plane. SEM images demonstrate the formation of highly ordered hexagonal nanorods with a crystallite sizes ranged from 40 to 500 nm depending on the film thickness. Optical measurements show transmittance of nearly 90% at low thicknesses (189.1µm) and about 60% for higher thickness (233.8 µm) with a calculated energy band gap values spanning from 2.85 to 3.20 eV. Photocatalytic activity is performed on selected ZnO samples have highly oriented nanorods with large hexagonal cross-section area. Photocatalytic activity takes placeon etched and as prepared ZnO film samples by monitoring photodegradation process of methylene blue MB using double beam spectrophotometer. Etched samples show higher photo activity than non- etched ones.

Keywords: ZnO thin films; Pulsed spray pyrolysis (PSP) technique; Selective etching; methylene blue (MB); Photocatalysis.

Introduction

Photocatalytic process depends mainly on exposing metal oxide semiconductor to UV, Visible light or combination of both. The photo excited electrons move to the conduction band leaving behind positive hole in the valence band. These photo generated electron / hole (e/h) pairs have the capability to reduce and/or oxidize the adsorbed toxic organic pollutant on the surface of the metal oxide photocatalyst. Photocatalytic activity of metal oxide photocatalyst stems from generation of $OH^{\bullet}$ & O_2^- radicals by the separated photo generated e/h pairs. Both radicals react with toxic pollutant to decompose or otherwise transform it to less harmful byproduct [1, 2].

Several metal oxides such as TiO_2, ZnO, SnO_2 and CeO_2 are reported in literature as photocatalyst [3-7]. To select the proper and high performance photocatalyst energy gap, separation and life time of photo generated e/h pairs, abundance and simple preparation technique should be considered [8-10].

Zinc oxide (ZnO) is one of the most important transparent conducting oxide semiconductors (II – IV) which are in the last few years attracted lot of concerns for many research groups due to its versatile applications. ZnO is an n-type semiconductor with a wide direct band gap in the range between 3 and 3.37 eV and large exciton binding energy of 60 meV, the existence of wide band gap is similar to some other and other nanomaterials[11-23].

There are three different crystalline forms for

*Corresponding author e-mail: as.abouelsayed@gmail.com; Tel: +201121727200
Received 8/ 11/2019; Accepted 3/12/2019
DOI: 10.21608/ejchem.2019.19253.2181

zinc oxide (ZnO) could be existed such as rock salt, cubic zinc blende and wurtzite (hexagonal structure) [24]. The most common ZnO crystalline structure is the wurtzite one which has high stability making it suitable forphotocatalytic and gas sensor applications [4]. Wurtzite structure [25,26] belongs to the C^4_{6V} spatial group since each one of Zn ions is surrounded by a tetragonal coordination which increases the polar symmetry over the hexagonal axis and this manifest a lot of different promising and interesting properties for ZnO.

Owing to its privilege with high transmittance in the visible region, highly electron mobility, chemical "nontoxic" and thermal stability, it is widely suitable to use in many applications such as transparent electrodes for light-emitting diodes (LEDs), photovoltaic cells, laser diodes, surface acoustic wave. In addition, it is used asheat mirrors, piezoelectric transducers, sterilization of medical equipment, promising substrate for immobilization of bio-molecules and biosensors transducer , UV- and gas sensors [27-34].

ZnO and other oxides materials such as MoO_3, WO_3, and VO_3 nano structured thin films and powders have been prepared by a wide variety of techniques, such as, pulsed (ablation) laser deposition (PLD or ALD)[35, 36], molecular beam epitaxy (MBE) [37], sputtering technique [38], electrochemical deposition [39], reactive evaporation [40], chemical vapor deposition (CVD) [41], sol-gel [42], and spray pyrolysis [43-49]. Among the preceding preparation techniques, spray pyrolysis is considered the most simple, large film scale, non- vacuum and inexpensive method[50, 51]. There are some other different ways to synthesis ZnO, which can be used in many applications [52-57]. The prepared films by spray pyrolysis technique depend on many different deposition parameters such as carrier gas type (nitrogen or air) and pressure, molarity of the precursor, deposition rate, substrate temperature, deposition time and nozzle to substrate distance. All of these parameters kept constant at their optimum values except the substrate temperature and deposition time are varied one at a time since they play crucial role in the characteristics of the deposited film. In principle ZnO thin film could be prepared with different techniques such as sputtering, thermal evaporation, laser ablation, sol gel, spray pyrolysis. Each technique has its own merit and drawback. Spray pyrolysis technique is used here since it is simple, vacuum less, system components are relatively cheap, the used chemical precursors have low cost.

There are many of homemade and fabricated spray systems which are different in designs and layout. Each of these has its own intimate effective parameters. Therefore, the properties of the same film deposited by each spray system are diversified.

The aim of this work is to prepare homogeneous, adhered, pin-hole and cracks free nanostructured ZnO thin film deposited at different times (film thickness) and different substrate temperatures on glass substrates by home-made rota table pulsed spray pyrolysis (PSP) system. The homogeneity, pin hole, cracks and adherence of the deposited films are checked by naked eyes and optical microscope. The dependence of structural, morphological and optical properties of deposited films is correlated with the different spray deposition times. Photocatalytic activity of ZnO films toward organic methylene blue (MB) is examined on a selected ZnO samples which has highly oriented nanorods with large cross-section area with and without selective etching.

Experimental

Zinc acetate dihydrate [Zn $(CH_3 (COO)_2 . 2H_2O]$, as the source for zinc atoms, is dissolved in a precalculated amount of ethyl alcohol (C_2H_5OH) and few drops of concentrated hydrochloric acid (HCl, 35%) as a stabilizer. The prepared mixture solution with molarity of (0.2 mol.) is stirred at room temperature for 60 min to yield a homogenous, transparent and clear solution. The glass substrates are cleaned ultrasonically using acetone, isopropanol and distilled water to prevent any lipids or chemisorption on the slides deposition surfaces.

Zinc oxide (ZnO) films areprepared by homemade pulsed spray pyrolysis (PSP) technique (Fig. 1) [50]. Rotatable (PSP) system with (On/ Off- mode) keeps the substrate temperature constant which promote the adhesion between the substrate and the deposited layers, permits enough time for film growth and homogeneity improvement. The substrate / nozzle distance isfixed at 30 cm with a solution flow rate of 5 ml / 2 min during different spray times (5, 10, 15, 20 and 25 minutes) with time interval of 5 seconds [2 sec. (On) and 3 sec. (Off) mode]. The substrate is heated at constant temperature (400, 450 or 500^{o}C). Compressed dry air pumped at a pressure of 2.5 bars to atomize the solution over the heated glass substrates.

The structural properties of the deposited samples are examined by Grazing angle X-ray diffraction technique (GAXRD - Diano corroboration-USA equipment with Cu K_α radiation of λ= 1.514 Å) to clarify the structure, crystallite size and to recognize the appeared phases of the investigated samples. The surface topography and film thickness are explored by scanning electron microscopy (SEM). Optical measurements (transmittance and reflectance spectra) are performed by double beam spectrophotometer (JASCO- 670 UV– VIS– NIR) in wavelength range from 0.2 to 2.5 µm. ZnO film deposited at 500°C and a spray time of 25 min is selected for selective etching by immersing the ZnO supported glass substrate in much diluted potassium hydroxide (KOH) solution of 50 mM for 5 minutes in water bath at 80°C. This chemical etching process is widely used because it is simple and efficient way to change the surface morphology of thin film structure [5, 6].Then, photocatalytic activities are evaluated for the etched and non-etched ZnO samples. Photodegradation test was executed by immersing both of the etched [6] and non-etched ZnO thin films into 5 ml of MB [$C_{16}H_{18}ClN_3S$] aqueous solution (10 mg/L) under illumination by a UV-pen lamp (λ_{max}= 254 nm and power 5 mW/cm^2). The change in MB absorbance was recorded using (Cary 100 UV-Vis) spectrophotometer.

Results and Discussion

Structural analysis

XRD

The structural properties of the deposited ZnO thin films were investigated by Grazing angle X-ray diffraction technique (GAXRD) to clarify the structure, crystallite size and to recognize the appeared phases of the prepared ZnO thin films. The XRD is very effective tool to explore the effect of spray time and the substrate temperature in the existence of polycrystalline nature in the deposited ZnO thin films. In general, the structural properties are varied with a variation in the preparation parameters of spray pyrolysis technique such as spray time, substrate temperature, as well as the doping concentration of starting reacting materials. The structural aspects of the deposited ZnO films at different substrate temperatures constant spray time (film thickness) and vice versa on glass substrates are elucidated by analyzing their XRD patterns are shown in Fig. (2 & 3). Only one peak with high intensity and others with lower intensities are appeared in the obtained patterns for samples deposited at 500°C while those deposited at 400°C & 450°C show a reasonable hump at 2θ =20°-32° range beside higher intensity one neighbored to another with lower intensity. These peaks are indexed with JCPDS files. It is found that these patterns are in good agreement with that reported in file number (No. # 36-1451). Based on, the investigated samples are only ZnO has a hexagonal polycrystalline nature with preferred orientation along (002) at 2θ≡ 34.5°.

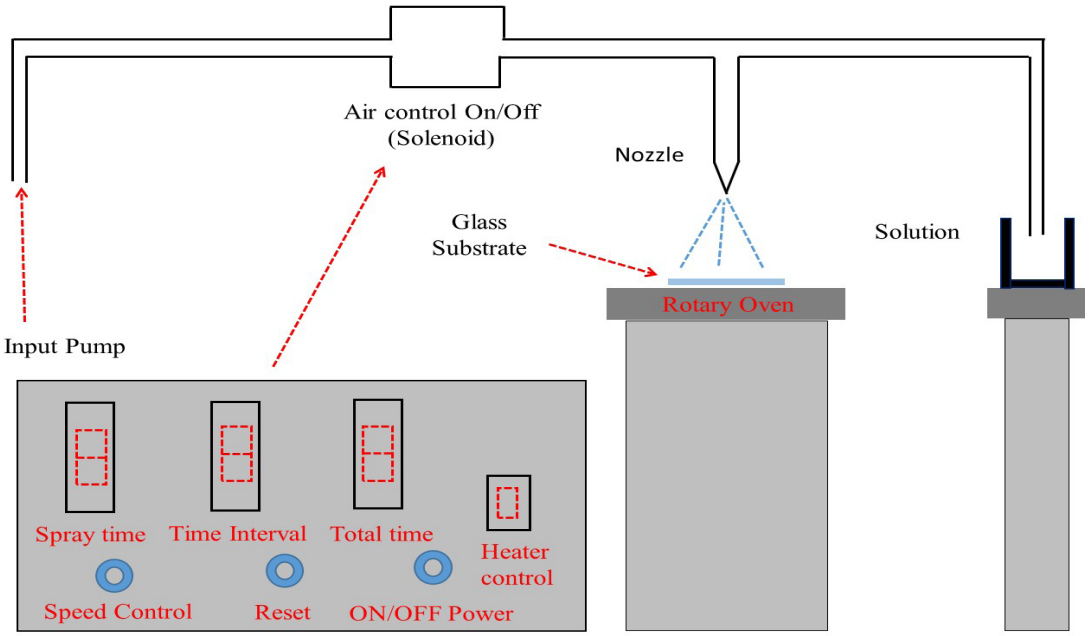

Fig. 1. Schematic diagram of pulsed spray pyrolysis (PSP) technique.

The observed hump at 2θ≈ 20 to 30° represents the overlap between the amorphous phase of ZnO, which decreases by increasing annealing temperature, and the amorphous glass substrate. ZnO has two peaks at 2θ (26°& 28° – JCPDS file No. #211486) which overlapped with the characteristic hump of the amorphous glass substrate. When the substrate temperature increase the high intensity peak corresponds to (002) and the lower intensity peaks correspond to (100), (101), (102), (103), (112) and (201) are appeared. Also, the intensity and number of appeared peaks are increased with increasing the deposition temperature. This may be due to the enhancement of crystallinity caused by the increase of atomic ordering.

Normally, the increase in deposition temperature of ZnO thin film allowing more ordering of the atoms ending with highly crystalline film as demonstrated by sample deposited at 500°C.

In order to explore the effect of spray time (film thickness) the substrate temperature 500°C was selected for depositing samples with different spray time since samples with good polycrystalline nature (Fig. 2) were deposited at this temperature. The covered spray time is ranged from 5 minutes up to 25 minutes with step of 5 minutes. The XRD patterns for these samples are displayed in Fig. 3. Only one peak with high intensity surrounded with two peaks have lower intensity and an obvious hump centered at 2θ=25°, which decreases with increasing spray time are observed for samples deposited at 500°C & 5 minutes spray time.

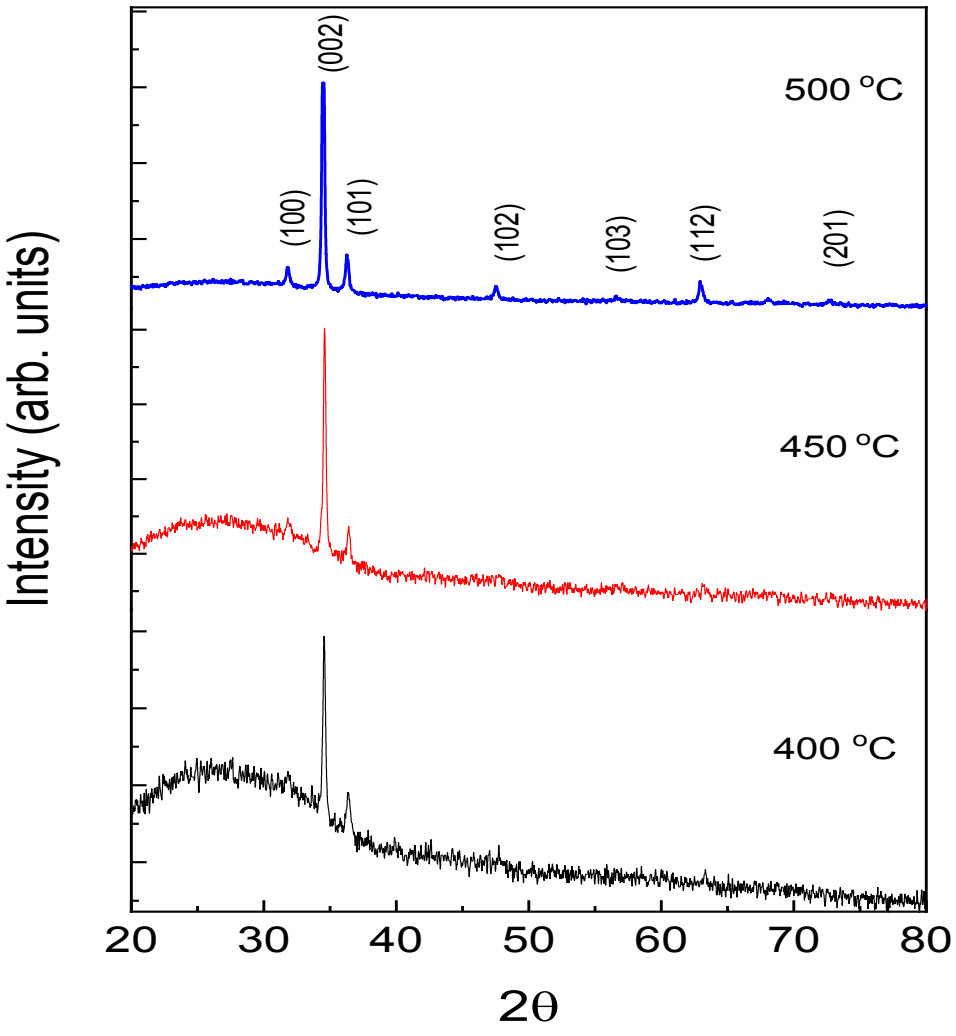

Fig. 2. XRD patterns of ZnO thin films deposited at different temperatures and constant spray time (25 min.).

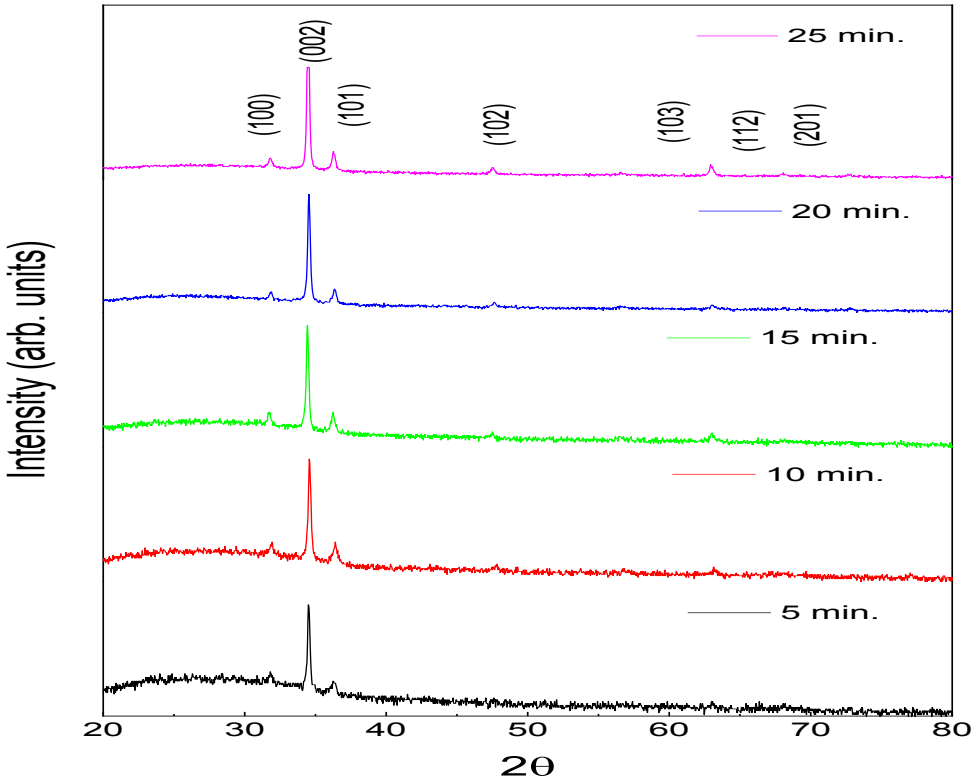

Fig. 3. XRD patterns of ZnO thin films deposited at different spray times (film thicknesses) at 500 °C.

The salient features related to an increase in spray time are reasonable increase in the high intense peak combined with slight change in intensity of the surrounded peaks and the tendency of the hump to be with lower intensity at 25 minutes. The full width at half maximum (FWHM) of the diffraction peak isused to determine the crystallite size (D) of the deposited films using Scherrer's formula [Eq.1][58]:

$$D = 0.9\lambda / \beta \cos\theta \qquad (1)$$

where D is the crystallite size, λ is the wavelength of X-ray (λ =0.15406 nm), β is the full width at half-maximum (FWHM), and θ is the half diffraction angle of the maximum observed peak (002). The strain ε values arecalculated from the following equation [Eq. 2] [59]:

$$\varepsilon = \left(c - c_o / c_o\right)100\% \qquad (2)$$

where, c is the lattice constant of ZnO thin films and c_0 the lattice constant of bulk standard (c_0 = 0.5206 nm) [43]. The calculated mean strain is found to be very small even with the increase in the crystallite size. This phenomenon was explained by Swapna et al. [60], they suggested that in sufficiently thicker films with more relaxed or less strained state as the number of film defects decreases the crystallinity improvement increases which reducing the films strain.

Spray time, film thickness (calculated from SEM micrographs cross section Fig. 5), crystallite size, calculated dislocation density ($\delta = 1/D^2$[61]) and strain *(ε)* of the deposited thin films reflects the increase and enhancement of the films crystallinity as the film is thicker. Moreover, the deposited film thickness and crystallite size found to be increases with increasing the spray time as shows in Fig. 4.

The idea pointed out by Swapna et al. [60] is that the crystallinity improvement increases means reducing the films strain. This can be due to in sufficiently thicker films as a results of increasing spray time the films appear with more relaxed or less strained state as the number of film defects decreases. The principle idea regarding to the effect of spray time is that the area of the particle cross-section and the gap between them increases with increasing the spray time which yields to the crystallinity improvement increases and reducing the films strain.

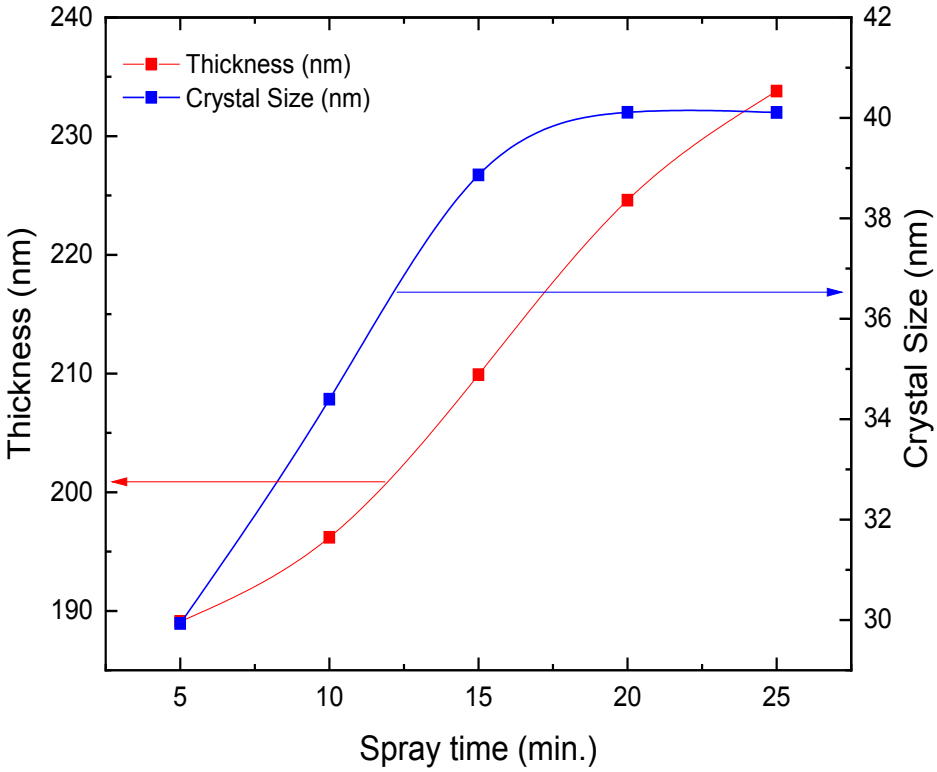

Fig. 4. Variation of film thickness & crystallite size at substrate temperature of 500 °C and different spray times.

Morphologic properties of ZnO thin films

The SEM images for ZnO films deposited at substrate temperature 500°C with different spray times ranging from 5 minutes up to 25 minutes with step 5 minutes are shown in Fig. 5.

The dependence of the crystallite size and crystallinity improvements on spray time (5, 10, 15, 20 & 25 min.) is salient feature. Morphological changes of the thin film structure arestarted from randomly distributed grains at 5 min., passing through agglomeration of small particles at 10 min., and finally forming homogeneous hexagonal cross-section for closely spaced particles.

As the spray time increases the area of the particle hexagonal cross-section and the gap between them increase which may increase the penetration and adsorption of the UV- light to be detected. This result makes the investigated sample a good candidate as an active material for UV- photocatalytic and degrading organic pollutants. The ZnO sample deposited at 500°C and spray time of 25 min was chosen for testing the etching effect because this sample showed a well oriented crystalline structure, well textured surface morphology high thickness and increased surface area.

Figure 6, represents the SEM images of the etched and non-etched samples. Presence of cracks and pores at the surface, sides and may be internally within the hexagonal nanorods in the etched samples is obvious. Such clefts in the thin film structure are expected to affect positively on the photocatalytic activity process.

Optical properties

As elucidated in Fig. 7; the pure ZnO thin films sprayed at different times show an optical transmittance which slightly exceeding 90% in the infra-red region and low transmittance percentage in the visible region. The disappearance of the significant interference oscillations in the optical curves may be due to highly roughness of the top surface of the prepared samples. The absorption edge (wavelength cut- off) value for all deposited layers due to the electronic transition between VB (valence band) and CB (conduction band) is ranged from 360 to 380 nm as shown in the inset graph of Fig. 7.,while the absorption in the visible region is related to the presence of some localized energy levels caused by intrinsic defects[43].

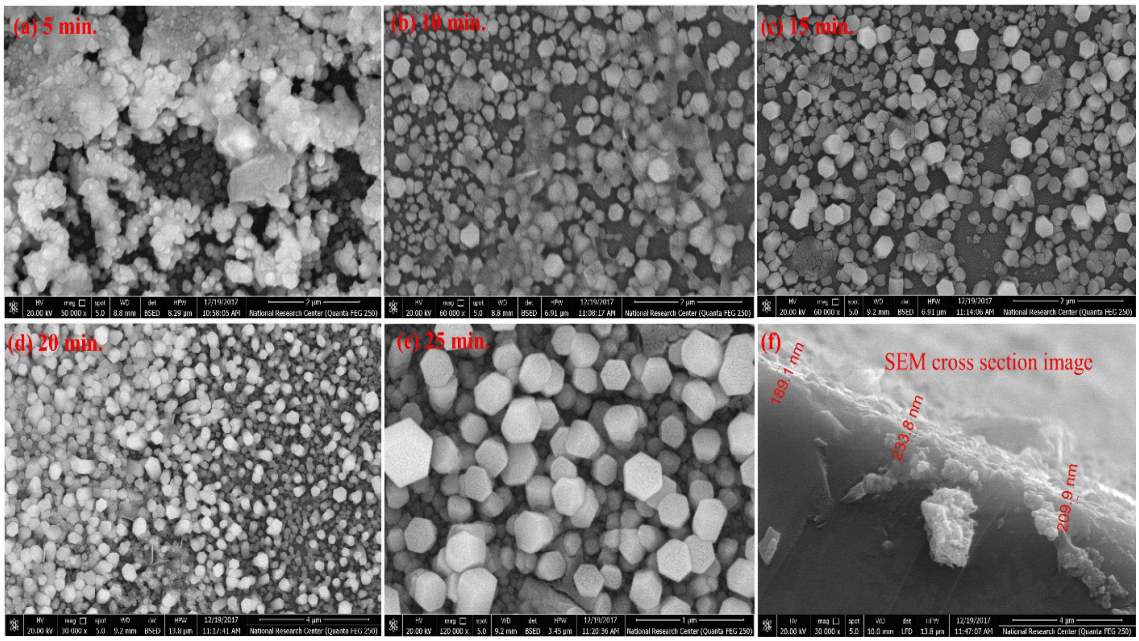

Fig. 5. SEM images of ZnO thin films at (5, 10, 15, 20 and 25 min.) at deposited temperature of 500 °C & typical tilt SEM micrograph cross section image.

The optical band gap energy was determined from the transmission spectra using the following equation [43]:

$$(\alpha h\nu)^2 = C(h\nu - E_g) \quad (3)$$

where, α is the absorption coefficient values, h is Planck's constant, ν is the radiation frequency, C is a constant, $h\nu$ is the photon energy and energy gap E_g of the semiconductor. $(\alpha h\nu)^2$ is traced versus $h\nu$to calculate the optical energy gap.

From this plot, the optical energy gap(E_g) is found to be from 2.85 to 3.2 eV, due to quantum size effect as shown in Fig. 8.The calculated value for the deposited sample at 5 min. is lower than the recorded values of the other deposited samples at (10, 15, 20 and 30 min.) which are more closer to the surveyed values of the energy band gap in literatures for the deposited ZnO films using the spray pyrolysis technique ranged between 3 to 3.37 eV [62,63]. This smaller value of the energy gap of the sample deposited at 5 min. could be attributed to the lower film thickness with smaller particle size and flagging of the crystallinity [62,63]. The refractive index of the deposited films is recorded to be between 1.8 –3; at photon energy values from 0.4 to 2.8 eV, respectively.These refractive index recorded values for the as deposited films are coincident with that reported in literature for the polycrystalline ZnO thin films [64].

Photocatalytic activity of ZnO thin films

Basically nanomaterials are uniquely characterized by their great surface area which is lost in bulk materials. Therefore nano size ZnO is promising for photodegradation since it has large surface area contacted with pollutant. The variation in absorbance spectra of methylene blue (MB) dye exposed at different times to UV- irradiation in presence ZnO thin films deposited at 500°C and spray time of 25 min is illustrated in Fig. 9. Both non-etched and etched samplesshow significant change in the MB absorbance as a result photodegradation. The degradation efficiency could be determined from the following equation [65]:

$$\text{Degradation (\%)} = \left(A_o - A/A_o\right) \times 100 \quad (4)$$

where A_o and A are the absorbance's at 664 nm of MB solution at the beginning of the reaction and after 45 min, respectively. The observed degradation efficiency after 45 min of illumination (99% and 96% for etched and non-etched samples, respectively) are of the highest recorded results for the immobilized photo-catalyst [66-68].

This observed slight difference in degradation efficiency could be attributed to the highly degradation rate at the starting time followed by slow rate along the degradation process for the etched samples [65-68]. Moreover, the relationship between the change in absorbance and the irradiation time was investigated in the

light of the first-order reaction kinetic model, which can be expressed as :

$$\ln\left(A/A_o\right) = -k_{app}\ t \qquad (5)$$

where, k_{app} is the apparent photocatalytic reaction rate constant, and t is the irradiation time. Validation of this model is shown in Fig. 10. The salient linear behavior emphasizes that the photodegradation process of MB organic dye over ZnO thin film can be considered as first order reaction. The calculated values of k_{app},0.14 min^{-1} and 0.07 min^{-1} for the etched and non- etched ZnO samples, respectively, are clearly indicate the superior photocatalytic activity of the etched sample. This might be due to the generation of new active sites in the formed slots on the cross-sectional area of the ZnOnanorods by etching which enhances the photocatalytic activity process [66-68].

It is worth mentioning that, all photocatalytic activity tests are performed three times on the only etched or non-etched ZnO films deposited at 500oC and spray time 25 minutes. The samples are cleaned after each exposure time by ethanol and distilled water for 5 min in an ultrasonic bath. The easy cleaning, fast recycling and quick response to UV- illumination reflect the high durability and long lifetime of these samples. The promotion of photocatalytic activity by simple process (etching) encourages application of immobilized ZnO film prepared by PSP system as an excellent photocatalyst for organic pollutant degradation and waste water treatment under UV-illumination. Selective etching phenomenon used here, we believe that it is highly effective in case of ZnO material since it has hexagonal structure. It is possible to obtain hollow hexagon of ZnO by attack the core across c-axes by selective etching inducing significant increase in surface area which increase the reaction probability.

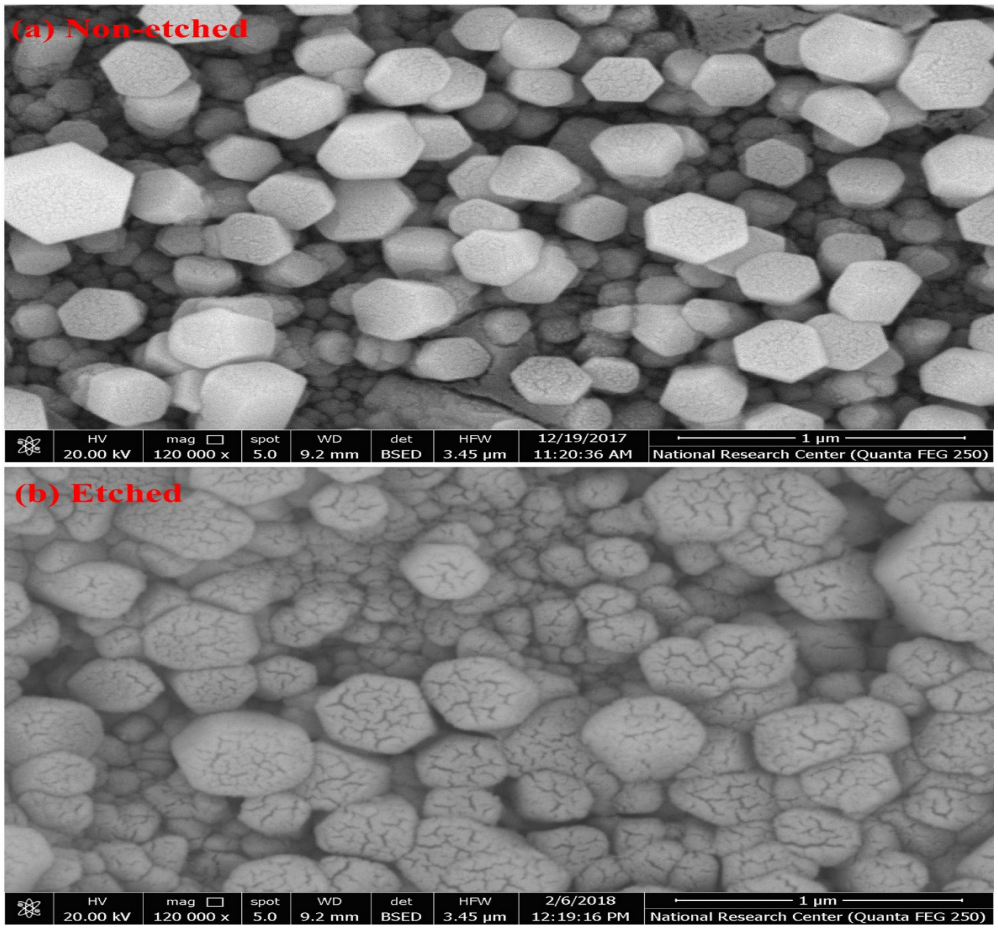

Fig. 6. SEM images for etched & non-etched ZnO thin films deposited at 500 °C and spray time of 25 min.

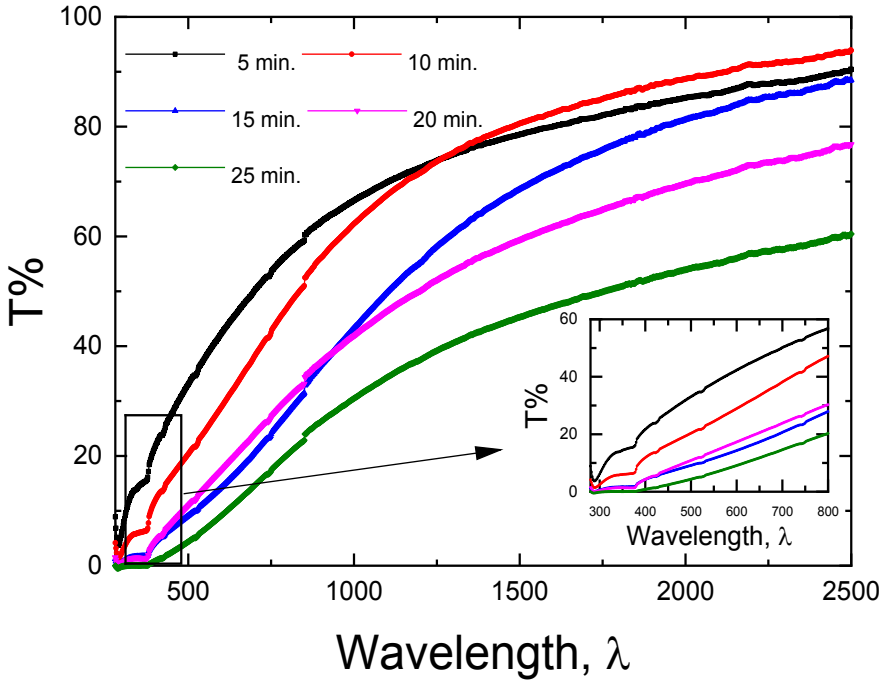

Fig. 7. Transmission spectra T(λ) of ZnO thin films as a function of deposition time (5,10, 15, 20 and 25 min.) at constant substrate temperature (500 °C).

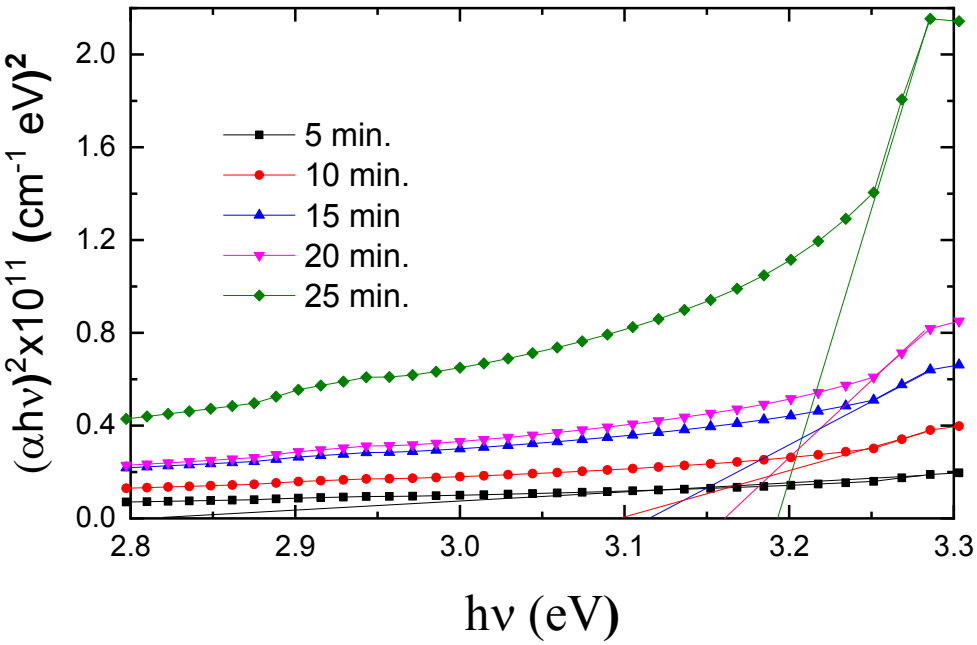

Fig. 8 . Plot of $(\alpha h\nu)^2$ vs. photon energy $h\nu$ for ZnO thin film as a function of deposition time (5, 10, 15, 20 and 25 min.) at constant substrate temperature (500 °C).

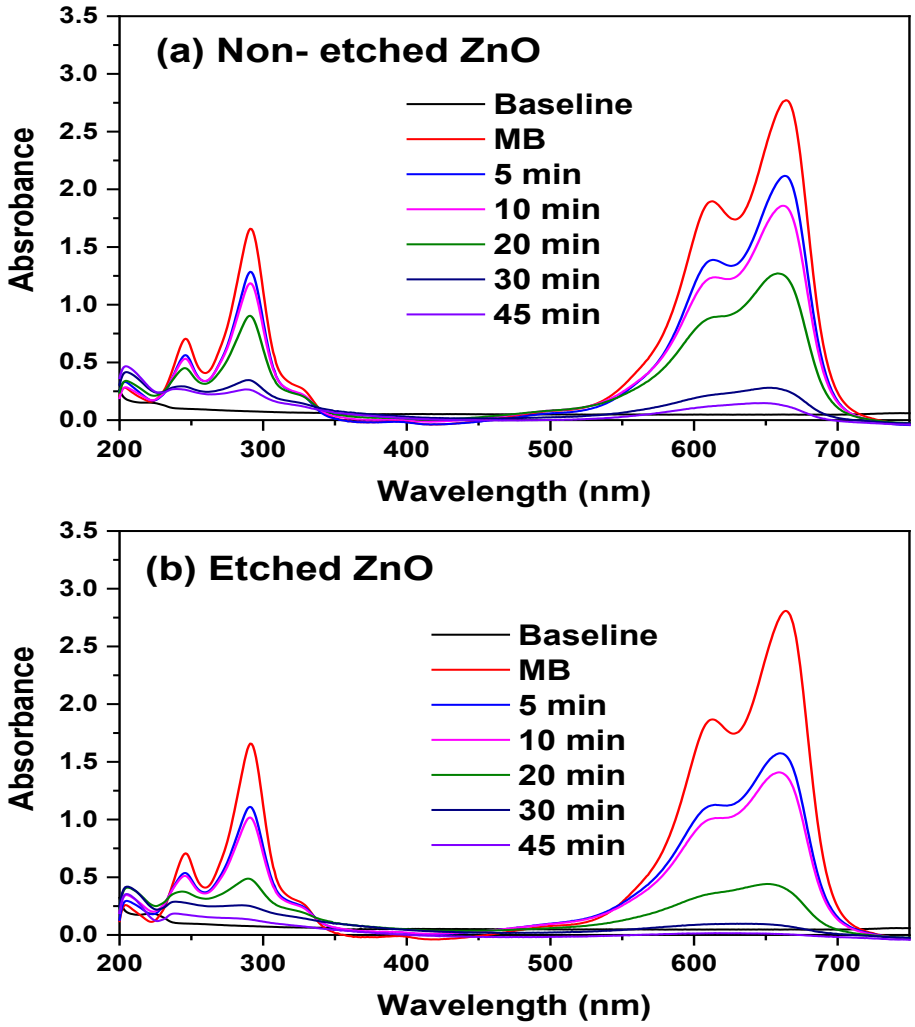

Fig. 9. Methylene blue (MB) absorption spectra of etched and non- etched ZnO films.

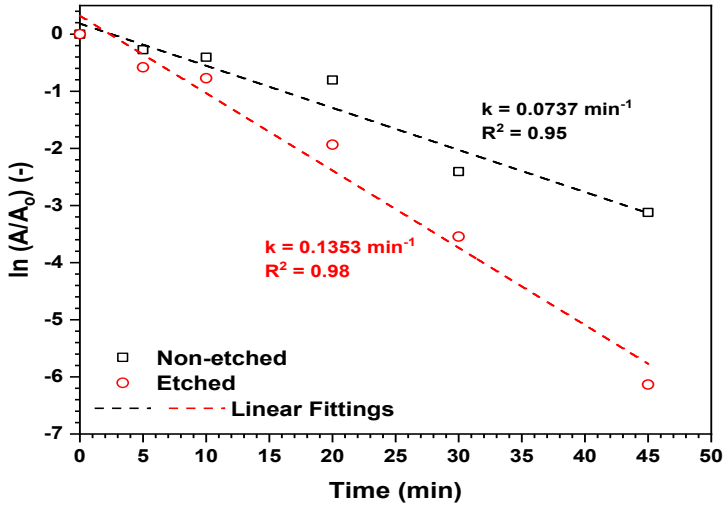

Fig. 10. The first order kinetics of methylene blue (MB) dye photo-degradation.

Conclusions

Pure nanostructured ZnO thin films are prepared on glass substrates at different deposition temperature and spray times by pulsed spray pyrolysis technique. XRD patterns elucidate the presence of preferential orientation along the c-axis along (002) plane. Crystallite size increases for the deposited ZnO with increasing the spray time from 5 to 25 min. SEM images show nano-hexagonal rods like structure for the deposited ZnO films at 500^{o}C and spray time of 25 minutes (working sample). Highly well ordered nanorod ZnO samples with a larger hexagonal cross-sectional area are selected to be etched by KOH which exhibits longitudinal slots. Photocatalytic activity process shows reasonable improvement. Optical measurements showed a transmission percentage about 90% with absorption band gap of 3.2 eV and well recorded refractive index which is compatible with the reported literature values. Photocatalytic activity experiments for the etched and non-etched ZnO films are performed employing methylene blue (MB) dye as a reference pollutant. Etched samples showed higher reaction rate constant than non-etched ones and recorded nearly 99% of dye degradation achievement after 45 minutes. This may be due to the generation of newly active sites in the formed hollow tubes after the etching process. Hence, the chemical etching process for ZnO thin films proved itself as a vital working method for photodegradation process enhancement in immobilized catalysis. According to these obtained results the prepared etched- ZnO thin films could be considered as a durable promising candidate for the photocatalytic treatment application of water pollutants.

Acknowledgements

The authors acknowledge with thanks the National Research Centre (NRC) for the technical and financial support.

Funding

This work was funded by King National Research Centre (NRC) under internal Project no. 11090331.

References

1. Hoffmann M.R., Martin S.T., Choi W. and Bahnemann D.W., Environmental applications of semiconductor photocatalysis. Chem Rev, 95, 69–96 (1995).
2. Hernández-Ramírez A. and Medina-Ramírez I., Photocatalytic semiconductors. Springer (2016).
3. Fujishima A. and Honda K., Electrochemical photolysis of water at a semiconductor electrode. Nature, 238, 37 (1972).
4. Grčić I., Papić S. and Brnardić I., Photocatalytic activity of TiO2 thin films: kinetic and efficiency study. Int J Chem React Eng, 16, 1 (2017).
5. Han K., Peng X.-L., Li F. and Yao M.-M., SnO2 composite films for enhanced photocatalytic activities. Catalysts, 8, 453 (2018).
6. Zhang J., Ding S., Yuan M., Tian X., Yin W., Ge Y., et al., The impact of heat treatment technology and parameters on TiO2 thin film forming, AIP Conference Proceedings, AIP Publishing, p. 020006 (2019).
7. Wang X., Jin Y. and Liang X., Significant photocatalytic performance enhancement of TiO2 by CeO2 atomic layer deposition, Nanotechnology, 28 (2017) 505709.
8. Pelizzetti E. and Minero C., Metal oxides as photocatalysts for environmental detoxification. Comments Inorgan Chem, 15, 297–337 (1994).
9. Hisatomi T., Kubota J. and Domen K., Recent advances in semiconductors for photocatalytic and photoelectrochemical water splitting. Chem Soc Rev, 43, 7520–7535 (2014).
10. Wang H., Zhang L., Chen Z., Hu J., Li S., Wang Z., et al., Semiconductor heterojunction photocatalysts: design, construction, and photocatalytic performances, Chem Soc Rev, 43, 5234–5244 (2014).
11. Bahadur L., Hamdani M., Koenig J. and Chartier P., Studies on semiconducting thin films prepared by the spray pyrolysis technique for photoelectrochemical solar cell applications: Preparation and properties of ZnO. Solar Energy Mater, 14, 107–120 (1986).
12. Choopun S., Vispute R., Noch W., Balsamo A., Sharma R. and Venkatesan T., et al., Oxygen pressure-tuned epitaxy and optoelectronic properties of laser-deposited ZnO films on sapphire, Appl Phys Lett, 75, 3947–3949 (1999).
13. Abouelsayed A., Thirunavukkuarasu K., Kamarás K., Hennrich F. and Kuntscher C.A., Pressure-induced phenomena in single-walled carbon nanotubes probed by infrared spectroscopy. High Pressure Res, 29, 559–563 (2009).
14. Abouelsayed A., Anis B., Hassaballa S., Khalil A., Rashed U.M., Eid K.A. and Al-Ashkar E., Preparation, characterization, Raman, and terahertz

spectroscopy study on carbon nanotubes, graphene nano-sheets, and onion like carbon materials. Mater Chem Phys, 189, 127–135 (2017).

15. Al-khattib M.G., Samir A., Ahmed M.A., Abouelsayed A. and Hassablla S., Spectroscopic studies to investigate the effect of different plasma parameters on the geometrical and electronic structure of graphene. Optics Laser Technol, 115, 433–440 (2019).
16. Ali S.S.M., Eisa W.H. and Abouelsayed A., Solvent-free and large-scale preparation of silver@ polypyrrole core@ shell nanocomposites; structural properties and terahertz spectroscopic studies. Compos Part B Eng, 176, 107289 (2019).
17. Aldeeb M.A., Morgan N., Abouelsayed A., Amin K.M. and Hassaballa S., Electrical and optical characterization of acetylene RF CCP for synthesis of different forms of hydrogenated amorphous carbon films. Plasma Chemistry and Plasma Processing (2019). Available at: https://doi.org/10.1007/s11090-019-10031-8
18. Aldeeb M.A., Morgan A.N., Abouelsayed A., Amin K.M. and Hassaballa S., Correlation of acetylene plasma discharge environment and the optical and electronic properties of the hydrogenated amorphous carbon films. Diamond Relat Mater, 96, 74–84 (2019).
19. Galal A.M.F., Atta D., Abouelsayed A., Ibrahim M.A. and Hanna A.G., Configuration and molecular structure of 5-chloro-N-(4-sulfamoylbenzyl) salicylamide derivatives. Spectrochim Acta Part A, 214, 476–486 (2019).
20. Gil B. and Kavokin A.V., Giant exciton-light coupling in ZnO quantum dots. Appl Phys Lett, 81, 748–750 (2002).
21. Marotti R., Guerra D., Bello C., Machado G. and Dalchiele E., Bandgap energy tuning of electrochemically grown ZnO thin films by thickness and electrodeposition potential. Solar Energy Mater Solar Cells, 82, 85–103 (2004).
22. Sahu D. and Huang J.-L., Development of ZnO-based transparent conductive coatings. Solar Energy Mater Solar Cells, 93, 1923–1927 (2009).
23. Xiong C., Yao R., Wan W. and Xu J., Fabrication and electrical characterization of ZnO rod arrays/CuSCN heterojunctions. Optik, 125, 785–788 (2014).
24. Saoud F.S., Plenet J.C. and Henini M., Band gap and partial density of states for ZnO: under high pressure. J Alloys Compounds, 619, 812–819 (2015).
25. Morkoç H., Index, Wiley Online Library 2009
26. Ojha A.K., Srivastava M., Kumar S., Hassanein R., Singh J., Singh M.K. and Materny A., Influence of crystal size on the electron–phonon coupling in ZnO nanocrystals investigated by Raman spectroscopy. Vib Spectrosc, 72, 90–96 (2014).
27. Benramache S., Temam H.B., Arif A., Guettaf A. and Belahssen O., Correlation between the structural and optical properties of Co doped ZnO thin films prepared at different film thickness. Optik, 125, 1816–1820 (2014).
28. Bretagnon T., Lefebvre P., Valvin P., Gil B., Morhain C. and Tang X., Time resolved photoluminescence study of ZnO/(Zn, Mg) O quantum wells. J Cryst Growth, 287, 12–15 (2006).
29. Delgado G.T., Romero C.Z., Hernández S.M., Pérez R.C. and Angel O.Z., Optical and structural properties of the sol–gel-prepared ZnO thin films and their effect on the photocatalytic activity. Solar Energy Mater Solar Cells, 93, 55–59 (2009).
30. El Jald E., Franiv V., Belayachi A. and Abd-Lefdil M., Optically stimulated piezooptical effects in Cu-doped ZnO films. Optik, 124, 6302–6304 (2013).
31. Fortunato E.M., Barquinha P.M., Pimentel A.C., Gonçalves A.M., Marques A.J., Martins R.F. and Pereira L.M., Wide-bandgap high-mobility ZnO thin-film transistors produced at room temperature. Appl Phys Lett, 85, 2541–2543 (2004).
32. Jiang X., Wong F., Fung M. and Lee S., Aluminum-doped zinc oxide films as transparent conductive electrode for organic light-emitting devices. Appl Phys Lett, 83, 1875–1877 (2003).
33. Lucio-Lopez M., Maldonado A., Castanedo-Perez R., Torres-Delgado G. and Olvera M.d.l.L., Thickness dependence of ZnO: in thin films doped with different indium compounds and deposited by chemical spray. Solar Energy Mater Solar Cells, 90, 2362–2376 (2006).
34. Park S., An S., Ko H., Lee S. and Lee C., Synthesis, structure, and UV-enhanced gas sensing properties of Au-functionalized ZnS nanowires. Sensors Actuators B, 188, 1270–1276 (2013).
35. Henkel B., Neubert T., Zabel S., Lamprecht C., Selhuber-Unkel C., Raetzke K., et al., Photocatalytic properties of titania thin films prepared by sputtering vs evaporation and aging

of induced oxygen vacancy defects. Appl Catal B, 180, 362–371 (2016).

36. Pérez-González M., Tomás S., Santoyo-Salazar J. and Morales-Luna M., Enhanced photocatalytic activity of TiO2-ZnO thin films deposited by dc reactive magnetron sputtering. Ceramics Int, 43, 8831–8838 (2017).

37. Bretagnon T., Lefebvre P., Guillet T., Taliercio T., Gil B. and Morhain C., Barrier composition dependence of the internal electric field in ZnO/Zn 1−x Mg x O quantum wells. Appl Phys Lett, 90, 201912 (2007).

38. Kim D., Shimomura T., Wakaiki S., Terashita T. and Nakayama M., Photoluminescence properties of high-quality ZnO thin films prepared by an RF-magnetron sputtering method. Phys B, 376, 741–744 (2006).

39. Karak N., Samanta P.K. and Kundu T.K., Green photoluminescence from highly oriented ZnO thin film for photovoltaic application. Optik, 124, 6227–6230 (2013).

40. Acharya A., Sarwan B., Panda R., Shrivastava S. and Ganesan V., Tuning of TCO properties of ZnO by silver addition. Superlattice Microst, 67, 97–109 (2014).

41. Maruyama T. and Shionoya J., Zinc oxide thin films prepared by chemical vapour deposition from zinc acetate. J Mater Sci Lett, 11, 170–172 (1992).

42. Zhao X., Li M. and Lou X., Sol–gel assisted hydrothermal synthesis of ZnO microstructures: morphology control and photocatalytic activity. Adv Powder Technol, 25, 372–378 (2014).

43. Aoun Y., Benhaoua B., Benramache S. and Gasmi B., Effect of deposition rate on the structural, optical and electrical properties of Zinc oxide (ZnO) thin films prepared by spray pyrolysis technique. Optik, 126, 2481–2484 (2015).

44. Bedia A., Bedia F.Z., Aillerie M., Maloufi N. and Benyoucef B., Morphological and optical properties of ZnO thin films prepared by spray pyrolysis on glass substrates at various temperatures for integration in solar cell. Energy Procedia, 74, 529–538 (2015).

45. Faraj M., Pakhuruddin M. and Taboada P., Structural and optical properties of cadmium sulfide thin films on flexible polymer substrates by chemical spray pyrolysis technique. J Mater Sci Lett, 28, 6628–6634 (2017).

46. Afify H.H., Hassan S.A., Abouelsayed A., Demian S.E. and Zayed H.A., Synthesis, characterization and structural control of nano crystalline molybdenum oxide MoO3 single phase by low cost technique. Mater Chem Phys, 176, 87–95 (2016).

47. Afify H.H., Hassan S.A., Abouelsayed A., Demian S.E. and Zayed H.A., Coloration of molybdenum oxide thin films synthesized by spray pyrolysis technique. Thin Solid Films, 623, 40–47 (2017).

48. Afify H.H., Hassan S.A., Obaida M., Moussa I. and Abouelsayed A., Preparation, characterization, and optical spectroscopic studies of nanocrystalline tungsten oxide WO3. Optics Laser Technol 111, 604–611 (2019).

49. Afify H.H., Hassan S.A., Obaida M. and Abouelsayed A., Influence of annealing on the optical properties of monoclinic vanadium oxide VO2 prepared in nanoscale by hydrothermal technique. Physica E, 114, 113610 (2019).

50. Obaida M., Moussa I. and Boshta M., Low sheet resistance F-doped SnO2 thin films deposited by novel spray pyrolysis technique. Int J ChemTech Res, 8, 239–247 (2015).

51. Obaida M., Moussa I., Hassan S., Demian S. and Afify H., Effect of TiO2 film thickness synthesized by pulse spray pyrolysis technique on the response to UV-illumination. Synthesis, 9, 10 (2019).

52. Ibrahim A.M., Abd El-Latif M.M. and Gohr M.S., Water/alcohol mediated preparation of ZnO hollow sphere. Egypt J Chem, 58, 475–484 (2015).

53. Ramadan M.A., Nassar S.H., Montaser A.S., El-Khatib1 E.M. and Abdel-Aziz M.S.. Synthesis of nano-sized zinc oxide and its application for cellulosic textiles. Egypt J Chem, 59, 523–535 (2016).

54. Mahmoud F.A., Elazab I., Abo-Elenien O.M., Abdel Fatah A. and Ahmed A.A.M.. Optical characterization of Poly [2-methoxy-5-(2-ethylhexyloxy-p-phenylene vinylene](MEH-PPV): C60, MEH-PPV: C60: TiO2 and MEHPPV: C60: ZnO thin films. Egypt J Chem, 62, 311–323 (2019).

55. Afify M., Samy N., Hafez N.A., Alazzouni A.S. and Kelany M.M., Evaluation of Zinc-oxide Nanoparticles effect on treatment of diabetes in streptozotocin-induced diabetic rats. Egypt J Chem, 62, 1771–1783 (2019).

56. Dief Allah M., Ali Z., Rozik N.N., Raslan M. and Sadek K.U., Electrical and mechanical properties of Nitrile rubber (NR) filled with industrial waste

and by product from manufacture of ferrosilicon alloys in Egyptian chemical industries company. Egypt J Chem, 60, 905–918 (2017).

57. Mwafy E.A., Dawy M., Abouelsayed A., Elsabbagh I.A. and Elfass M.M., Synthesis and Characterization of Multi-Walled Carbon Nanotubes Decorated ZnO Nanocomposite. Egypt J Chem, 59, 1061–1068 (2016).
58. Klung H. and Alexander L., X-ray diffraction procedures. Wiles, New York, 687 (1974).
59. Benramache S. and Benhaoua B., Influence of substrate temperature and Cobalt concentration on structural and optical properties of ZnO thin films prepared by Ultrasonic spray technique. Superlattices Microstruct, 52, 807–815 (2012).
60. Swapna R., Ashok M., Muralidharan G. and Kumar M.S., Microstructural, electrical and optical properties of ZnO: Mo thin films with various thickness by spray pyrolysis. J Anal Appl Pyrolysis, 102, 68–75 (2013).
61. Kose S., Atay F., Bilgin V. and Akyuz I., In doped CdO films: electrical, optical, structural and surface properties. Int J Hydrogen Energy, 34, 5260–5266 (2009).
62. El Sayed A., Taha S., Said G. and Yakuphanoglu F., Controlling the structural and optical properties of nanostructured ZnO thin films by cadmium content. Superlattices Microstruct, 65, 35–47 (2014).
63. Demian S., Optical and electrical properties of transparent conducting ZnO films prepared by spray pyrolysis. J Mater Sci Lett, 5, 360–363 (1994).
64. Shan F. and Yu Y., Band gap energy of pure and Al-doped ZnO thin films. J Eur Ceramic Soc, 24, 1869–1872 (2004).
65. Bizarro M. and Martínez-Padilla E., Visible light responsive photocatalytic ZnO: Al films decorated with Ag nanoparticles. Thin Solid Films, 553, 179–183 (2014).
66. Duta M., Perniu D. and Duta A., Photocatalytic zinc oxide thin films obtained by surfactant assisted spray pyrolysis deposition. Appl Surf Sci, 306, 80–88 (2014).
67. Stambolova I., Blaskov V., Shipochka M., Vassilev S., Petkova V. and Loukanov A., Simple way for preparation of ZnO films by surfactant mediated spray pyrolysis. Mater Sci Eng B, 177, 1029–1037 (2012).
68. Huang J., Liu S., Kuang L., Zhao Y., Jiang T., Liu S. and Xu X., Enhanced photocatalytic activity of quantum-dot-sensitized one-dimensionally-ordered ZnO nanorod photocatalyst. J Environ Sci, 25, 2487–2491 (2013).